



DOI: <http://dx.doi.org/10.1590/1807-1929/agriambi.v25n4p264-269>

Sensor system for acquisition of vegetation indexes¹

Sistema sensor para aquisição de múltiplos índices de vegetação

Thales M. de A. Silva^{2*} , Domingos S. M. Valente² , Francisco de A. de C. Pinto² ,
Daniel M. de Queiroz²  & Nerilson T. Santos³ 

¹ Research developed at Universidade Federal de Viçosa, Departamento de Engenharia Agrícola, Laboratório de Projeto de Máquinas e Visão Artificial (PROVISAGRO), Viçosa, MG, Brasil

² Universidade Federal de Viçosa/Departamento de Engenharia Agrícola, Viçosa, MG, Brazil

³ Universidade Federal de Viçosa/Departamento de Estatística, Viçosa, MG, Brazil

HIGHLIGHTS:

A sensor based on phototransistors was developed to measure crop vegetation indexes.

The NDVI, SR, WDRVI, SAVI, and OSAVI vegetation indexes were obtained.

The results obtained using the developed sensor were similar to those obtained using a spectroradiometer.

ABSTRACT: Vegetation indexes are important indicators of the health and yield of agricultural crops. Among the sensors used to evaluate vegetation indexes, proximal sensors can be used for real-time decision-making. Thus, the objective of this study was to develop a proximal sensor system based on phototransistors to acquire and store the following vegetation indexes: normalized difference vegetation index, simple ratio, wide dynamic range vegetation index, soil-adjusted vegetation index, and optimized soil-adjusted vegetation index. The sensor system was developed using an analog circuit to acquire reflectance data from red and near-infrared bands. The sensor system was calibrated according to the results of a spectroradiometer, using *Zoysia japonica* grass as the target. An algorithm that calculates and stores vegetation indexes in a file was developed. The Pearson correlation between the vegetation indexes obtained with the sensor system and the spectroradiometer was evaluated. The vegetation indexes presented a Pearson correlation higher than 0.92 to the estimated values by the spectroradiometer. Under the evaluation conditions, the proposed sensor system could be used to determine all vegetation indexes evaluated.

Key words: precision agriculture, phototransistor, reflectance, proximal sensing

RESUMO: Os índices de vegetação são importantes indicadores da saúde e produtividade das culturas agrícolas. Dentre os tipos de sensores, os sensores proximais podem ser utilizados para tomada de decisão em tempo real. Dessa forma, o objetivo deste estudo foi desenvolver um sistema sensor proximal, com base em fototransistor, para obtenção e armazenamento dos índices de vegetação: NDVI (Índice de Vegetação da Diferença Normalizada), SR (Razão Simples), WDRVI (Índice de Vegetação de Larga Escala Dinâmica), SAVI (Índice de Vegetação Ajustado ao Solo) e OSAVI (Índice de Vegetação Ajustado ao Solo Otimizado). O sistema sensor foi desenvolvido utilizando um circuito analógico para realizar a aquisição de dados de reflectância das bandas do vermelho e infravermelho próximo. O sistema sensor foi calibrado, utilizando grama *Zoysia japonica*, para ajustar seus valores aos de um espectroradiômetro. Desenvolveu-se um algoritmo que calcula os índices de vegetação e armazena os resultados em um arquivo. Avaliou-se a correlação de Pearson entre os índices de vegetação obtidos com o sistema sensor e o espectroradiômetro. Os índices de vegetação apresentaram correlação de Pearson superiores a 0,92 com os valores estimados pelo espectroradiômetro. Nas condições analisadas, o sistema sensor proposto pode ser utilizado na determinação de todos os índices de vegetação abordados.

Palavras-chave: agricultura de precisão, fototransistor, reflectância, sensoriamento proximal

• Ref. 232515 – Received 24 Dec, 2019

* Corresponding author - E-mail: thalesmaurino@gmail.com

• Accepted 22 Dec, 2020 • Published 03 Feb, 2021

Edited by: Carlos Alberto Vieira de Azevedo

This is an open-access article distributed under the Creative Commons Attribution 4.0 International License.



INTRODUCTION

Vegetation indexes are important indicators of biomass (Yue et al., 2019), soil parameters (Bernardi et al., 2017), plant chlorophyll content (Xu et al., 2019), plant cover (Shao et al., 2016), and plant leaf area (Ricci et al., 2019). Vegetation indexes include the normalized difference vegetation index (NDVI; Rouse Jr. et al., 1973), simple ratio (SR; Jordan, 1969), wide dynamic range vegetation index (WDRVI; Gitelson, 2004), soil-adjusted vegetation index (SAVI; Huete, 1988), and optimized soil-adjusted vegetation index (OSAVI; Rondeaux et al., 1996).

Vegetation indexes can be calculated using images acquired from orbital (Zhang & Roy, 2016; Mengue et al., 2019) and sub-orbital (Ghazal et al., 2015; Zheng et al., 2016) platforms such as remotely piloted aircrafts. However, both data collection platforms present limitations. Orbital platforms may present a low frequency of data acquisition, low spatial resolution, and loss of information in images due to cloud cover. Some remotely piloted aircraft may present high cost and low flight autonomy. In addition, both approaches require the processing of images after collection (Matese et al., 2015).

Proximal sensors are an alternative to orbital and sub-orbital sensors; they can be used manually or coupled to agricultural tractors (Pallottino et al., 2019). These sensors have the advantage of estimating crop vegetation indexes in real time; thus, decisions such as fertilizer dosage for variable rate application can be made at the same time as when the vegetation indexes are estimated.

New sensors have been developed using phototransistors as sensor devices to determine soil and vegetation attributes (O'Toole & Diamond, 2008; Mukherjee & Laskar, 2019). Phototransistors are electronic components that vary the electrical resistance according to the incident light intensity. Phototransistors can be calibrated based on electrical resistance to determine the reflectance of crops. Thus, the objective of this study was to develop a proximal sensor system based on phototransistors that operate in the red and near-infrared ranges to acquire and store the following vegetation indexes: NDVI, SR, WDRVI, SAVI, and OSAVI.

MATERIAL AND METHODS

The development of the sensor system was divided into four phases. First, an analog circuit was used to acquire reflectance data from red and near-infrared bands. Second, the sensor system was calibrated using data acquired with a spectroradiometer (FieldSpec® HandHeld 2; Analytical Spectral Devices, Boulder, USA). Third, an algorithm was developed from the data collected by the analog circuit to calculate and store the vegetation indexes. Fourth, Pearson correlation analysis was carried out for the vegetation indexes obtained with the sensor system and the spectroradiometer.

The sensor system of the vegetation indexes was developed using an analog circuit composed of phototransistors as sensor devices. The phototransistors used were the Everlight PT334-6C and the Fairchild QSD124, which capture the red and near-infrared bands, respectively. The Everlight PT334-6C capture a spectral range from 400 to 1,100 nm, with sensitivity

peak at 940 nm; thus, to obtain the red band reflectance, a band-pass filter that selectively transmitted the red band radiation to the detection surface of the phototransistor was installed. The band-pass filter for the red band had a bandwidth at half-maximum (FWHM) curve of 66 nm and sensitivity peak at 679 nm, according to measures of the spectroradiometer. The Fairchild QSD124 phototransistor had an encapsulation with a band-pass filter for infrared, with a sensitivity peak at 880 nm; thus, it did not require an additional filter.

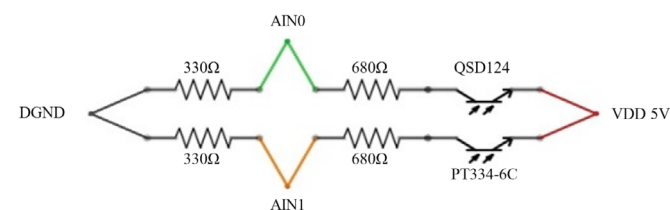
The signal reading and processing was carried out using a single-board computer BeagleBone Black (BBB) Review C (BeagleBoard.org Foundation, Oakland, USA, BeagleBoard, 2019), with the operating system Debian 7.8 Wheezy. This single-board computer was chosen because of its low cost and because it allows for the rapid development of new tools for precision agriculture (Olesen et al., 2016).

The signal was received through the AIN0 and AIN1 analog ports of the BBB. These ports operate with analog signals of voltages from 0 to 1.8 V. Considering that the phototransistors operate at 5 V, a voltage divisor circuit was required for the BBB to read the signal. This circuit was built with 680 and 330 Ω resistors arranged in series to each phototransistor (Figure 1). The use of this circuit resulted in a variation of 0-1.63 V in the resistor of 330 Ω , which is compatible with the analog ports of the BBB.

The built analog circuit was protected by a 120 \times 57 \times 32-mm black plastic box (width \times depth \times height). According to the manufacturer, the phototransistor Fairchild QSD124 has a light reception angle of approximately 12°, whereas the manufacturer of the Everlight PT334-6C did not specify the reception angle, which was considered to be approximately 12° in the present study. Thus, a black cone was inserted in front of each phototransistor to ensure that the lateral light would have no effect (Figure 2).

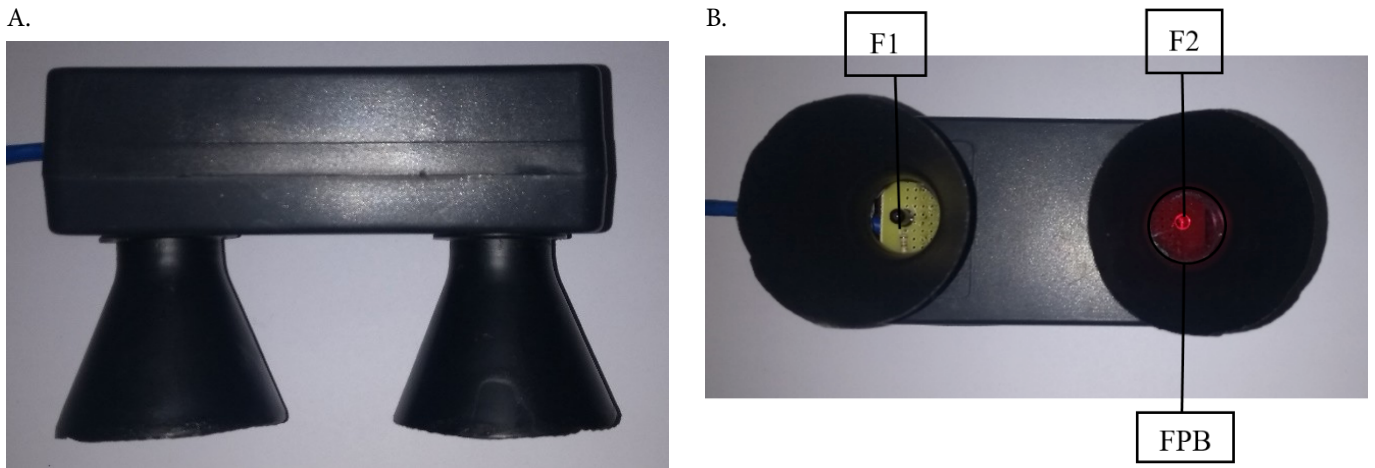
The reflectance data of the proposed sensor system was calibrated using data from the spectroradiometer. The reflectance of four Spectralon targets, with reflectance of 0.00 (0%), 0.50 (50%), 0.75 (75%), and 1.00 (100%), were used as reference for this calibration. These targets were circular with a diameter of 0.05 m.

Considering that the light reception angle of the phototransistors was approximately 12° and that the targets had a diameter of 0.05 m, 0.10 m of distance between the targets and the sensor system was adopted to ensure that the phototransistors received only the reflectance of the calibration targets. The spectroradiometer was calibrated for the same distance using the Spectralon target with a reflectance of 1.00 (100%). Sixty readings with the proposed sensor system were performed for each target. The average of the 60 readings



AIN0 and AIN1 = analog ports of the BeagleBone Black (BBB); VDD 5V = voltage of 5 V of the BBB; DGND = voltage of 0 V of the BBB

Figure 1. Diagram of the analog circuit of the sensor system



F1 = phototransistor that captures the near-infrared band, Fairchild QSD124; F2 = phototransistor that captures the red band, Everlight PT334-6C; FPB = band-pass filter of red; A = lateral view; B = bottom view

Figure 2. Sensor system developed to obtain the red and near-infrared bands to calculate the vegetation indexes (NDVI, SR, WDRVI, SAVI, and OSAVI)

of the sensor system for each target and the readings of the spectroradiometer were subjected to linear regression.

The calibration was done in a 1.30 × 1.00 × 0.70-m black box (width × depth × height) using a 650-W halogen lamp for illumination and was placed at 0.80 m of distance from the target to control the environmental light conditions. The reflectance in the red and near-infrared bands obtained by the sensor system were compared to the average reflectance measured by the spectroradiometer in the range of 674-684 nm and 875-885 nm, respectively.

An algorithm was developed in the C++ language, using the Qt Creator 4.0.2 program as an integrated development environment. In the algorithm, the signals received from the analog circuit were interpreted to obtain the reflectance in the red and near-infrared bands. Before obtaining the reflectance values, the Spectralon targets were read with a reflectance of 1.00 (100%). This reading was used as a reference value in Eqs. 1 and 2:

$$R = \frac{R_1}{R_2} \tag{1}$$

where:

- R - reflectance in the red band;
- R₁ - red band signal reflected by the object; and,
- R₂ - red band signal of the reference (measured red band reflectance of the Spectralon target).

$$NIR = \frac{NIR_1}{NIR_2} \tag{2}$$

where:

- NIR - reflectance in the near-infrared band;
- NIR₁ - near-infrared band signal reflected by the object; and,
- NIR₂ - near-infrared band signal of the reference (measured near-infrared reflectance of the Spectralon target).

The reflectance obtained in Equations 1 and 2 was used to determine the vegetation indexes: NDVI, according to

Eq. 3 (Rouse et al., 1973), SR, according to Eq. 4 (Jordan, 1969), WDRVI, according to Eq. 5 (Gitelson, 2004), SAVI, according to Eq. 6 (Huete, 1988), and OSAVI, according to Eq. 7 (Rondeaux et al., 1996):

$$NDVI = \frac{NIR - R}{NIR + R} \tag{3}$$

$$SR = \frac{NIR}{R} \tag{4}$$

$$WDRVI = \frac{a \cdot NIR - R}{a \cdot NIR + R} \tag{5}$$

where:

- a - weighting coefficient.

The range of the weighting coefficient of the WDRVI (a) is from 0.00 to 1.00, where 1.00 is a WDRVI equal to NDVI. The coefficient value usually used to calculate the WDRVI is 0.2 (Xue & Su, 2017); this was the value used in the present study.

$$SAVI = \frac{NIR - R}{NIR + R + L} (1 + L) \tag{6}$$

where:

- L - soil adjustment factor.

The range of the soil adjustment factor of the SAVI (L) is from 0.00 to 1.00, where 0.00 is a SAVI equal to NDVI. The adjustment factors commonly used are 0.25 for high vegetation density, 0.50 for medium vegetation density, and 1.00 for low vegetation density (Hishe et al., 2017). A value of L = 0.5 works well for most situations and is a standard value (Lu et al., 2015); this value was used in the present study for the calculations using the spectroradiometer and the sensor system.

The OSAVI is a particular case of SAVI in which the soil adjustment factor (L) is defined as 0.16.

$$\text{OSAVI} = \frac{\text{NIR} - \text{R}}{\text{NIR} + \text{R} + 0.16} (1 + 0.16) \quad (7)$$

Vegetation indexes of 30 sample units of *Zoysia japonica* grass were obtained with the sensor system and the spectroradiometer. These sample units were rectangular, with dimensions of 0.30 × 0.15 m. The sample units and the order of the readings were randomly selected. The conditions used for the readings were the same as those used for calibration of the sensor system.

The data obtained by the sensor system and the spectroradiometer were subjected to linear regression using the Fisher's F test to obtain R² values. Pearson correlation analysis was used to compare the vegetation indexes obtained with the sensor system with the estimated values with the spectroradiometer.

RESULTS AND DISCUSSION

The linear regression for the reflectance obtained with the sensor system and the spectroradiometer showed R² values higher than 0.98 for the red and 0.99 for the infrared bands (Figure 3). These results corroborate the findings of Ryu et al. (2010) and Garrity et al. (2010), who developed spectral sensors with light emitting diodes and photodiodes and found R² higher than 0.94.

According to the F test ($p \leq 0.05$), the reflectance of the red and infrared bands obtained from the sensor system and the spectroradiometer were statistically equal. Thus, no linear equations of regression models in the algorithm of the sensor system were required to adjust the results to the values of the spectroradiometer.

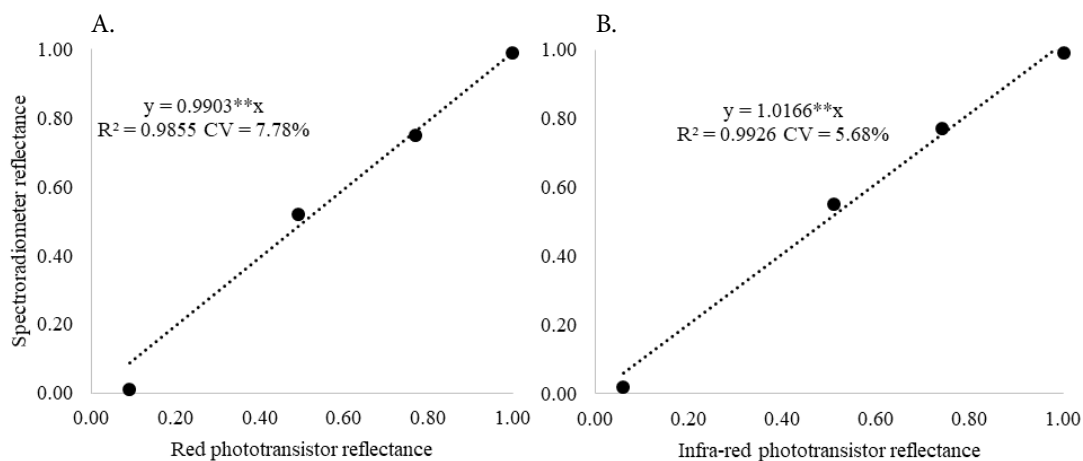
The vegetation indexes obtained using the spectroradiometer and the sensor system presented a high correlation (Figure 4), showing a Pearson correlation higher than 0.92 for all vegetation indexes, at a significance level of $p \leq 0.01$.

The values of the NDVI, SR, and WDRVI indexes obtained using the sensor system were closer to those found using the spectroradiometer than the results of the other vegetation indexes. NDVI presented the lowest Pearson correlation, despite being one of the indexes that presented the highest similarity between the sensor system and the spectroradiometer. SR presented a higher range of variation

than the other vegetation indexes evaluated, and it changed from 1.98 to 3.79. This result was expected because SR is the only index that is not normalized and, thus, presents no saturation problems and is more sensitive to high values of plant cover (Galvanin et al., 2014). The WDRVI presented a higher range of variation than the NDVI, showing that it was more sensitive than NDVI for the R and NIR reflectance values obtained in the samples. This is due to the normalization procedure used in the NDVI, which makes it insensitive to variations in NIR band reflectance, when it is much higher than R band reflectance. Under these conditions, the values of the numerator and the denominator of the NDVI equation are almost the same, and the sensitivity of the index to increases in NIR band reflectance becomes insignificant (Gitelson, 2004).

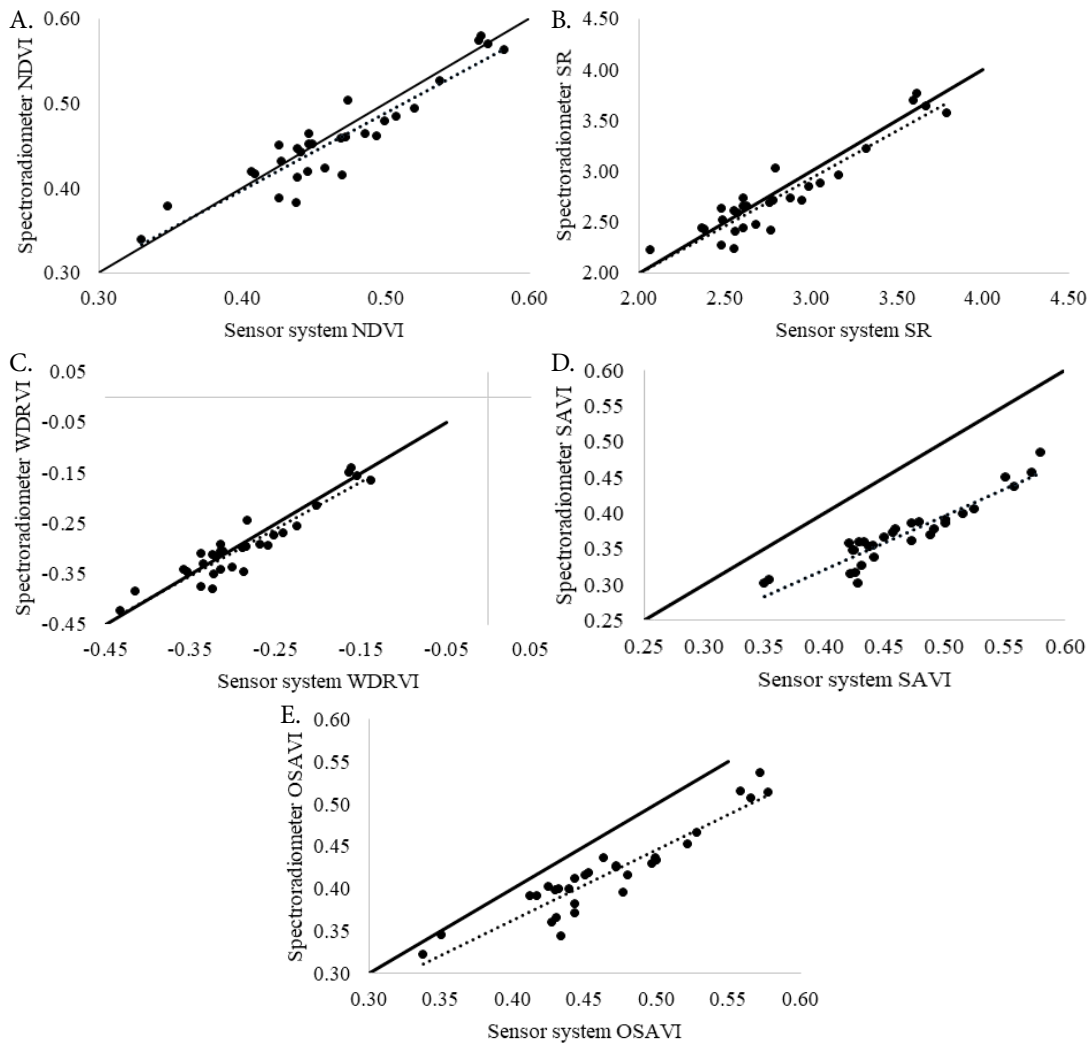
The data of the sensor system for the SAVI and OSAVI indexes remained overestimated in relation to the indexes calculated by the spectroradiometer. SAVI and OSAVI are used to decrease the effect of the soil in vegetation evaluations (Candiago et al., 2015); thus, they modify the origin of the R and NIR bands through their *L* factors (0.5 and 0.16, respectively) (Huete, 1988). The *L* factor overestimated the values of the SAVI and OSAVI indexes in the sensor system in relation to the values of the spectroradiometer (Figures 4D and 4E) due to differences in the sensitivity of each sensor in the R and NIR bands. The sensor system presented higher absolute values of the R and NIR bands than those of the spectroradiometer. Although the spectra of the spectroradiometer and the sensor system were similar when using Spectralon targets, they presented variations when using *Z. japonica* grass, which affected the measurements of the devices. The change caused by the *L* factor increased the slope of the line formed by the ratio used, thus increasing the difference between the means of the vegetation indexes adjusted to soil for the sensor system in relation to the spectroradiometer.

The *L* factor is a fixed value that differently affected the data of the two devices because the values of the R and NIR bands measured by each sensor were different when using the grass, despite the initial calibration. Therefore, the *L* factor generated a systematic error when applied to the denominator of the equation and increased this systematic error in the multiplication. The impact of the *L* factor was found in SAVI and OSAVI (Figures 4D and 4E). The *L* factor of the SAVI was



** = Significant at $p \leq 0.01$ by the F test

Figure 3. Calibration of reflectance of red (A) and infrared (B) bands obtained from the spectroradiometer



** = significant at $p \leq 0.01$ by the t test; straight line (—) = $(x = y)$; dots (●) = values found; dotted line (...) = fitted model; r = Pearson coefficient of correlation

Figure 4. Correlation between vegetation indexes obtained using the spectroradiometer and the sensor system: (A) NDVI, normalized difference vegetation index; (B) SR, simple ratio; (C) WDRVI, wide dynamic range vegetation index; (D) SAVI, soil-adjusted vegetation index; and (E) OSAVI, optimized soil-adjusted vegetation index.

defined as 0.50, higher than that for the OSAVI ($L = 0.16$); thus, it was more distant from the $x = y$ line. Another form used to observe this systematic error caused by the L factor was to make the L value equal to 0. In this case, the SAVI and OSAVI values were equal to the NDVI, and the values of the two sensors became more similar, as seen in Figure 4A.

CONCLUSIONS

1. The determination of the red and near-infrared reflectance using the developed sensor system was possible after calibrating it using Spectralon targets.

2. The proposed sensor system could be used to determine NDVI, SR, WDRVI, SAVI, and OSAVI vegetation indexes because the results for the indexes presented high and significant correlation with those of the spectroradiometer under the conditions evaluated.

ACKNOWLEDGEMENTS

The present study was conducted with the support of the Coordenação de Aperfeiçoamento de Pessoal de Nível Superior

(CAPES; Financing Code 001), the Conselho Nacional de Desenvolvimento Científico e Tecnológico (CNPq) and the Fundação de Amparo à Pesquisa do Estado de Minas Gerais (FAPEMIG).

LITERATURE CITED

- BeagleBoard. Beaglebone Black. In: What is Beaglebone Black? 2019. Available on: <<https://beagleboard.org/black>>. Accessed on: Mar. 2019.
- Bernardi, A. C. de C.; Grego, C. R.; Andrade, R. G.; Rabello, L. M.; Inamasu, R. Y. Spatial variability of vegetation index and soil properties in an integrated crop-livestock system. *Revista Brasileira de Engenharia Agrícola e Ambiental*, v.21, p.513-518, 2017. <http://dx.doi.org/10.1590/1807-1929/agriambi.v21n8p513-518>
- Candiago, S.; Remondino, F.; De Giglio, M.; Dubbini, M.; Gattelli, M. Evaluating multispectral images and vegetation indices for precision farming applications from UAV images. *Remote Sensing*, v.7, p.4026-4047, 2015. <https://doi.org/10.3390/rs70404026>

- Galvanin, E. A. S.; Neves, S. M. A. S.; Cruz, C. B. M.; Neves, R. J.; de Jesus, P. H. H.; Kreitlow, J. P. Avaliação dos Índices de Vegetação NDVI, SR e TVI na discriminação de fitofisionomias dos ambientes do Pantanal de Cáceres/MT. *Ciência Florestal*, v.24, p.707-715, 2014. <http://dx.doi.org/10.5902/1980509815729>
- Garrity, S. R.; Vierling, L. A.; Bickford, K. A simple filtered photodiode instrument for continuous measurement of narrowband NDVI and PRI over vegetated canopies. *Agricultural and Forest Meteorology*, v.150, p.489-496, 2010. <https://doi.org/10.1016/j.agrformet.2010.01.004>
- Ghazal, M.; Al Khalil, Y.; Hajjdiab, H. UAV-based remote sensing for vegetation cover estimation using NDVI imagery and level sets method. In: 2015 IEEE International Symposium on Signal Processing and Information Technology (ISSPIT), p.332-337, 2015. <https://doi.org/10.1109/ISSPIT.2015.7394354>
- Gitelson, A. A. Wide dynamic range vegetation index for remote quantification of biophysical characteristics of vegetation. *Journal of Plant Physiology*, v.161, p.165-173, 2004. <https://doi.org/10.1078/0176-1617-01176>
- Hishe, S.; Lyimo, J.; Bewket, W. Effects of soil and water conservation on vegetation cover: a remote sensing based study in the Middle Suluh River Basin, northern Ethiopia. *Environmental Systems Research*, v.6, p.26, 2017. <https://doi.org/10.1186/s40068-017-0103-8>
- Huete, A. R. A soil-adjusted vegetation index (SAVI). *Remote Sensing of Environment*, v.25, p.295-309, 1988. [https://doi.org/10.1016/0034-4257\(88\)90106-X](https://doi.org/10.1016/0034-4257(88)90106-X)
- Jordan, C. F. Derivation of leaf-area index from quality of light on the forest floor. *Ecology*, v.50, p.663-666, 1969. <https://doi.org/10.2307/1936256>
- Lu, L.; Kuenzer, C.; Wang, C.; Guo, H.; Li, Q. Evaluation of three MODIS-derived vegetation index time series for dryland vegetation dynamics monitoring. *Remote Sensing*, v.7, p.7597-7614, 2015. <https://doi.org/10.3390/rs70607597>
- Matese, A.; Toscano, P.; Di Gennaro, S.; Genesio, L.; Vaccari, F.; Primicerio, J.; Belli, C.; Zaldei, A.; Bianconi, R.; Gioli, B. Intercomparison of UAV, aircraft and satellite remote sensing platforms for precision viticulture. *Remote Sensing*, v.7, p.2971-2990, 2015. <https://doi.org/10.3390/rs70302971>
- Mengue, V. P.; Fontana, D. C.; Silva, T. S. da; Zanotta, D.; Scottá, F. C. Methodology for classification of land use and vegetation cover using MODIS-EVI data. *Revista Brasileira de Engenharia Agrícola e Ambiental*, v.23, p.812-818, 2019. <http://dx.doi.org/10.1590/1807-1929/agriambi.v23n11p812-818>
- Mukherjee, S.; Laskar, S. Vis-NIR-based optical sensor system for estimation of primary nutrients in soil. *Journal of Optics*, v.48, p.87-103, 2019. <https://doi.org/10.1007/s12596-019-00517-1>
- Olesen, D.; Jakobsen, J.; Benzon, H. H.; Knudsen, P. GNSS Software Receiver for UAVs. *European Journal of Navigation*, 6p. June 2016.
- O'Toole, M.; Diamond, D. Absorbance based light emitting diode optical sensors and sensing devices. *Sensors*, v.8, p.2453-2479, 2008. <https://doi.org/10.3390/s8042453>
- Pallottino, F.; Antonucci, F.; Costa, C.; Bisaglia, C.; Figorilli, S.; Menesatti, P. Optoelectronic proximal sensing vehicle-mounted technologies in precision agriculture: A review. *Computers and Electronics in Agriculture*, v.162, p.859-873, 2019. <https://doi.org/10.1016/j.compag.2019.05.034>
- Ricci, G. F.; Romano, G.; Leronna, V.; Gentile, F. Effect of check dams on riparian vegetation cover: A multiscale approach based on field measurements and satellite images for leaf area index assessment. *Science of the Total Environment*, v.657, p.827-838, 2019. <https://doi.org/10.1016/j.scitotenv.2018.12.081>
- Rondeaux, G.; Steven, M.; Baret, F. Optimization of soil-adjusted vegetation indices. *Remote Sensing of Environment*, v.55, p.95-107, 1996. [https://doi.org/10.1016/0034-4257\(95\)00186-7](https://doi.org/10.1016/0034-4257(95)00186-7)
- Rouse Jr., J.; Haas, R. H.; Schell, J. A.; Deering, D. W. Monitoring vegetation systems in the Great Plains with ERTS. In: Third ERTS Symposium, NASA, v.351, p.309-317, 1973.
- Ryu, Y.; Baldocchi, D. D.; Verfaillie, J.; Ma, S.; Falk, M.; Ruiz-Mercado, I.; Hehn, T.; Sonnentag, O. Testing the performance of a novel spectral reflectance sensor, built with light emitting diodes (LEDs), to monitor ecosystem metabolism, structure and function. *Agricultural and Forest Meteorology*, v.150, p.1597-1606, 2010. <https://doi.org/10.1016/j.agrformet.2010.08.009>
- Shao, Y.; Lunetta, R. S.; Wheeler, B.; Iiames, J. S.; Campbell, J. B. An evaluation of time-series smoothing algorithms for land-cover classifications using MODIS-NDVI multi-temporal data. *Remote Sensing of Environment*, v.174, p.258-265, 2016. <https://doi.org/10.1016/j.rse.2015.12.023>
- Xu, M.; Liu, R.; Chen, J. M.; Liu, Y.; Shang, R.; Ju, W.; Wu, C.; Huang, W. Retrieving leaf chlorophyll content using a matrix-based vegetation index combination approach. *Remote Sensing of Environment*, v.224, p.60-73, 2019. <https://doi.org/10.1016/j.rse.2019.01.039>
- Xue, J.; Su, B. Significant remote sensing vegetation indices: A review of developments and applications. *Journal of Sensors*, 2017, Article ID 1353691. <https://doi.org/10.1155/2017/1353691>
- Yue, J.; Yang, G.; Tian, Q.; Feng, H.; Xu, K.; Zhou, C. Estimate of winter-wheat above-ground biomass based on UAV ultrahigh-ground-resolution image textures and vegetation indices. *ISPRS*, v.150, p.226-244, 2019. <https://doi.org/10.1016/j.isprsjprs.2019.02.022>
- Zhang, H. K.; Roy, D. P. Landsat 5 Thematic Mapper reflectance and NDVI 27-year time series inconsistencies due to satellite orbit change. *Remote Sensing of Environment*, v.186, p.217-233, 2016. <https://doi.org/10.1016/j.rse.2016.08.022>
- Zheng, H.; Zhou, X.; Cheng, T.; Yao, X.; Tian, Y.; Cao, W.; Zhu, Y. Evaluation of a UAV-based hyperspectral frame camera for monitoring the leaf nitrogen concentration in rice. In: 2016 IEEE International Geoscience and Remote Sensing Symposium (IGARSS), p.7350-7353, 2016. <https://doi.org/10.1109/IGARSS.2016.7730917>